

## Order-Disorder Transition in $\text{Na}_{0.25}\text{TiO}_2$ Bronze: Thermodynamic and Crystallographic Studies\*

L. BROHAN,† R. MARCHAND, AND M. TOURNOUX

*Laboratoire de Chimie des Solides, U.A. 279, Université de Nantes, 2, rue de la Houssinière, 44072 Nantes Cedex 03, France*

Received March 9, 1987

A stoichiometric Wadsley bronze  $\text{Na}_{0.25}\text{TiO}_2$  has been prepared for the first time. The perovskite-like sites of the  $\text{TiO}_2$  framework are fully occupied by sodium ions. The space group, at room temperature, is  $P2/a$  or  $Pa$  and the lattice parameters are  $a = 12.177(3) \text{ \AA}$ ,  $b = 3.875 \times 4 = 15.50(2) \text{ \AA}$ ,  $c = 6.480(3) \text{ \AA}$ ,  $\beta = 107.08(2)^\circ$ . As compared with those of the well-known Wadsley bronze of  $C2/m$  symmetry, X-ray and electron diffraction patterns exhibit extra reflections at about  $b^*/4$ . At  $T_c^{3D} = 430 \text{ K}$ , a second-order transition appears. The smooth variation of the  $\eta$ -order parameter and the anomalous specific heat have been studied. The critical exponents  $\alpha \approx \alpha' = 0.110 \pm 0.003$  and  $\beta = 0.324$  are in good agreement with those calculated from renormalization group method for  $d = 3$  and  $n = 1$  ( $d =$  dimensionality and  $n =$  number of order parameter components). © 1988 Academic Press, Inc.

### Introduction

Review articles (1-3) dealing with the properties of bronzes show that while the tungsten bronzes, at all temperatures, are metals, the vanadium ones exhibit semiconducting behavior and that the molybdenum bronzes, including the so-called "blue bronze"  $A_{0.30}\text{MoO}_3$  ( $A = \text{K, Rb, Tl}$ ) exhibiting a metal-semiconductor transition, seem to be intermediate in properties with respect to  $d$ -electron localization and the width of the conduction band (4-6).

Metal-semiconductor transitions are observed for some stoichiometric ratios corresponding to a particular filling of the conduction band. The properties of such compounds are mostly determined by anisotropic Fermi surfaces with nesting prop-

erties leading to charge density wave (CDW) instabilities.

The  $\text{Ti}^{III}$   $3d$ -electron is not as firmly bound as that of  $\text{V}^{IV}$ , so it was of interest to examine whether a Peierls transition could occur in titanium bronzes of particular stoichiometries and also to attempt the preparation of  $\text{Na}_{0.25}\text{TiO}_2$ .

Physical properties of titanium bronzes have already been studied, including that of the spinel phase  $\text{Li}_{1+x}\text{Ti}_{2-x}\text{O}_4$  which, in the composition range  $0 < x < 0.1$ , exhibits superconductivity at 11 K (7-10), but attention has never been focused on particular stoichiometry such as  $x = 0.25$  in  $\text{Na}_x\text{TiO}_2$ . The  $\text{Na}_x\text{TiO}_2$  crystal structure with  $0.20 < x < 0.235$  has been determined by Wadsley to be in the  $C2/m$  space group (11, 12).

The bronze with  $x = 0.25$ , in which the perovskite-like sites are fully occupied by sodium ions, has been prepared. It crystallizes, at room temperature, in the  $P2/a$  (or

\* Dedicated to John B. Goodenough.

† To whom all correspondence should be addressed.

*Pa*) space group with the lattice parameters  $a = 12.177(3)$  Å,  $b = 3.875 \times 4 = 15.50(2)$  Å,  $c = 6.480(3)$  Å,  $\beta = 107.08(2)^\circ$ . Its physical and structural properties are quite different from those of the Wadsley bronzes (13, 14). Its electrical and magnetic behavior will be described in a forthcoming paper (15). The initial results on the thermodynamic and crystallographic properties are presented here.

### Synthesis

$A_xMO_n$  bronzes are generally prepared two ways (3):

reaction of appropriate mixtures of  $MO_n$ ,  $M$  (or  $MO_{n-1}$ ), and  $AO_m$  or

removal of oxygen from  $AO_m$ ,  $MO_n$  mixtures by spontaneous decomposition or chemical or electrolytic reductions.

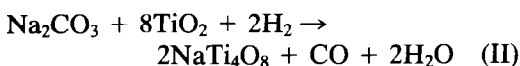
The Wadsley bronze  $Na_{0.20}TiO_2$  (11) has been prepared by reduction of  $Na_2Ti_3O_7$  under hydrogen at 1225 K for 2 days. The product obtained is a mixture of several black phases.  $Na_{0.20}TiO_2$  is isolated after dissolution of the unidentified compounds by boiling for several days in hydrofluoric and sulfuric acids.

Reid and Sienko (13) prepared  $Na_xTiO_2$  ( $0.20 < x < 0.235$ ) by heating a stoichiometric mixture of  $Na_2Ti_3O_7$ , Ti, and  $TiO_2$  for 12 to 40 hr at 1200 K in a platinum-sealed tube.

$x = 0.235$  is the highest  $x$  value obtained in the earlier synthesis of the Wadsley bronze at high temperatures. Attempts to reach the particular ratio  $x = 0.25$  were carried out through three different chemical reactions:



as in the Reid and Sienko method.



in which the finely ground mixture of the solid phases was heated in an alumina cru-

cible for 15 hr at 1300 K under a hydrogen stream.



in which sodium and titanium dioxide were heated for 12 hr at 1600 K in a nickel tube sealed under vacuum and this tube heated at the same temperature under an atmosphere of argon before use.

The starting materials were titanium dioxide (Merck 99.99%), sodium carbonate (R.P. 99.5%), sodium (Merck >99%), titanium powder (Merck 99.9%).

All three methods produced homogeneous blue-black products, acicular crystals for the first, powders for the second, and small platelet-like crystals for the third. For a better understanding, in connection with their preparation methods, these three bronzes will be hereafter referenced as type I, II, and III, respectively.

### Analysis

Only the type II bronze has been chemically analyzed, after dissolution in hot concentrated sulfuric acid, by absorption spectrophotometry for Na and a colorimetric method for Ti (a). It is almost impossible to dissolve the type I and III crystals completely; their sodium and titanium contents were determined by using the CASTAING microprobe technique (b). They are consistent with the results inferred from the structural determinations (c). The results are presented in Table I where a, b, and c refer to the analysis technique used.

TABLE I

Reaction type	<i>T</i> (K)	Duration (hr)	Na/Ti molar ratio
I	1200	24	$0.235 \pm 0.009$ (b)
	1300	36	$0.206 \pm 0.003$ (c)
II	1200	12-40	$0.249 \pm 0.008$ (a)
III	1600	12	$0.253 \pm 0.008$ (b)
			$0.248 \pm 0.003$ (c)

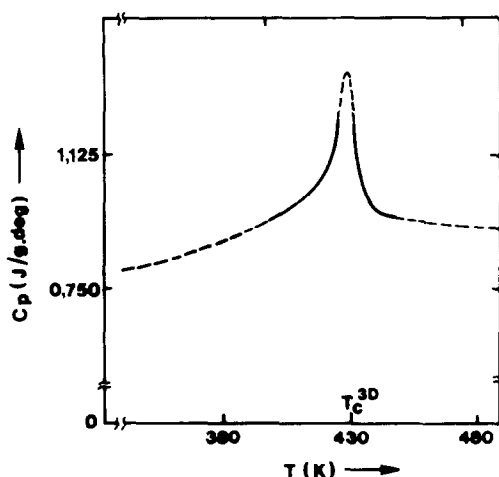


FIG. 1. Anomalous specific heat. Dotted line, experimental results; solid line, simulated curve by  $(T_c - T)^{-\alpha}$  and  $(T - T_c)^{-\alpha'}$ .

## Results and Discussion

### Specific Heat Anomaly

The specific heat was calculated from enthalpy measurements using a differential scanning calorimeter (DSC 4 Perkin-Elmer) with a linear rise of temperature. The thermal analysis produced evidence for Na<sub>0.25</sub>TiO<sub>2</sub> (type II and III) at  $T = 430$  K, a reversible phase transition.

The anomalous specific heat observed (Fig. 1) is characteristic of a second-order transition which has been simulated, as shown by the full line in Fig. 1, by  $(T_c - T)^{-\alpha}$  below  $T_c$  and  $(T - T_c)^{-\alpha'}$  above  $T_c$ , with  $\alpha \approx \alpha'$ . The critical exponent  $\alpha$  (Table II) is in good agreement with that calculated from the renormalization group method for

$d = 3$  and  $n = 1$  ( $d =$  dimensionality,  $n =$  number of order parameter components),  $\alpha = \alpha' = 0.111 \pm 0.0045$  (16).

### Electron Diffraction

Transmission electron diffraction experiments have been performed from room temperature to 800 K using a JEOL 100 CX (120 kV) electron microscope. The side entry stage allows a tilt angle of  $\pm 60^\circ$  with the standard specimen holder and one of  $\pm 45^\circ$  with the heating specimen holder.

The reciprocal lattice exploration of Na<sub>0.206</sub>TiO<sub>2</sub> (type I) by tilting around **b** indicates that the reciprocal lattice corresponds to that of the ordinary bronze structure  $C2/m$  (Fig. 2).

Figure 3a shows the (001)\* plane common to the two other bronzes (types II and III). It may be described as a periodic arrangement of the main lattice reflections with extra reflections near  $b^*/4$ . The strongest superreflections correspond to odd  $k$  values and the weakest ones to even  $k$  values such as  $k = 2(2n + 1)$ . These two types of superlattice reflections also appear in the (102)\* plane (Fig. 4) for the lines with  $k = 3, 5, 11, 13, \dots$ , and  $k = 2, 6, 10, 14, \dots$ , respectively. An explanation of the relative spot positions is obtained from the drawing of the tridimensional reciprocal lattice (Fig. 5).

The observed superlattice reflections may be due to a periodic modulation involving small atomic displacements from the average structure. In the commensurate phase, the wave vector **Q** of the modulation is  $\mathbf{Q} = \pm \mathbf{a}^* \pm q\mathbf{b}^* \pm 0\mathbf{c}^*$ , with  $q \approx 0.25$ . The resulting Fermi wave vector ( $q = 2k_F$ ),  $k_F \approx 0.125$  is concordant with the conducting properties of this compound (15) and with the 1/4 filling of the conduction band. The weakest superlattice reflections are related to the Bragg spots by  $\mathbf{Q}' = \pm 2\mathbf{a}^* \pm 2q\mathbf{b}^* \pm 0\mathbf{c}^*$ . The second-order satellites indicate that the modulation is not purely sinusoidal (17, 18).

TABLE II

$T_c^{3D}$ (K)	$430 \pm 1$
$\Delta T$ (K)	375–460.5
$\Delta T/T$	0.20
$\Delta H$ (J g <sup>-1</sup> )	$4.89 \pm 0.05$
$\Delta C_p/C_p\%$	28
$\alpha$	$0.107 \pm 0.003$
$\alpha'$	$0.110 \pm 0.003$

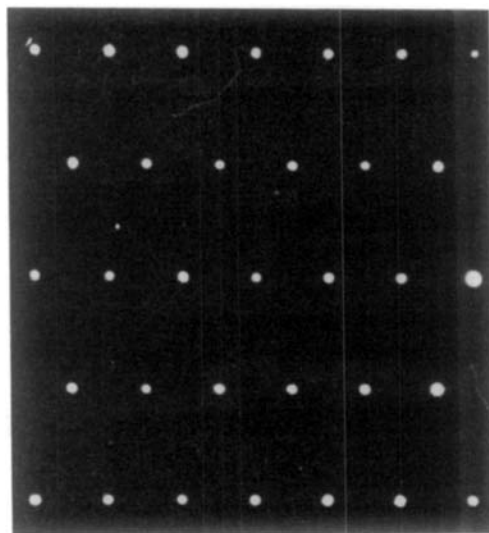
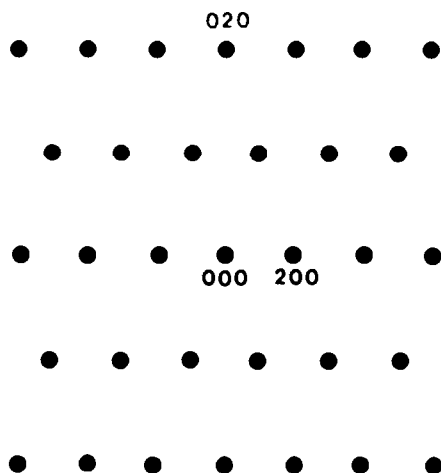


FIG. 2. Electron diffraction pattern:  $(001)^*$  plane for  $\text{Na}_{0.206}\text{TiO}_2$  type I and for  $\text{Na}_{0.25}\text{TiO}_2$  types II and III at elevated temperature.

When the temperature increases, the  $Q$  component along  $\mathbf{b}^*$  decreases, the superlattice becoming incommensurate with respect to the main lattice reflections. This decrease in  $q = 0.25 - \varepsilon$  and the intensity of the superlattice reflections are related: the second-order satellites are the first to disappear (Fig. 3b), then the first-order ones vanish, leaving only the  $C2/m$  main lattice (Fig. 2).

The temperature dependence of  $q$  cannot be investigated by electron diffraction experiments since electron beam irradiation induces local heating of the sample, making it difficult to determine the transition temperature precisely. The value obtained in such experiments is systematically lower than that given by differential scanning calorimetry and X-ray diffraction.

#### X-Ray Diffraction

The X-ray scattering experiments were performed first at room temperature by usual photographic methods in order to characterize the two sublattices and then with an automatic Nonius CAD4 diffractometer.

The existence condition on  $h0l$ ,  $h = 2n$ , implies that the low-temperature commensurate phase belongs to the  $P2/a$  or  $Pa$  space group.

In order to determine the  $q$  component of the wave vector modulation along  $\mathbf{b}^*$ , the lattice parameters of a type III crystal were studied at room temperature. Prior to this study, three sets of reflections were selected from the electron diffractions patterns according to the temperature dependence of the  $\mathbf{q}$  vector. The first one contained superreflections with  $k = 1, 5, 9, \dots$ , the second with  $k = 3, 7, 11, \dots$ , and the last with the main lattice reflections. The parameters calculated from these three sets and the corresponding  $q$  values are reported in Table III.

The linewidths of the Bragg peaks and of the satellites are identical, in accord with the long-range order at this temperature. As mentioned earlier only the  $Q$  component along  $\mathbf{b}^*$  is affected and assumes a  $q$  value of  $0.24915 \pm 0.0005$ ; the Fermi wave vector  $k_F$  is then 0.1245.

The temperature dependence of  $q$  was studied by the precession method with non-

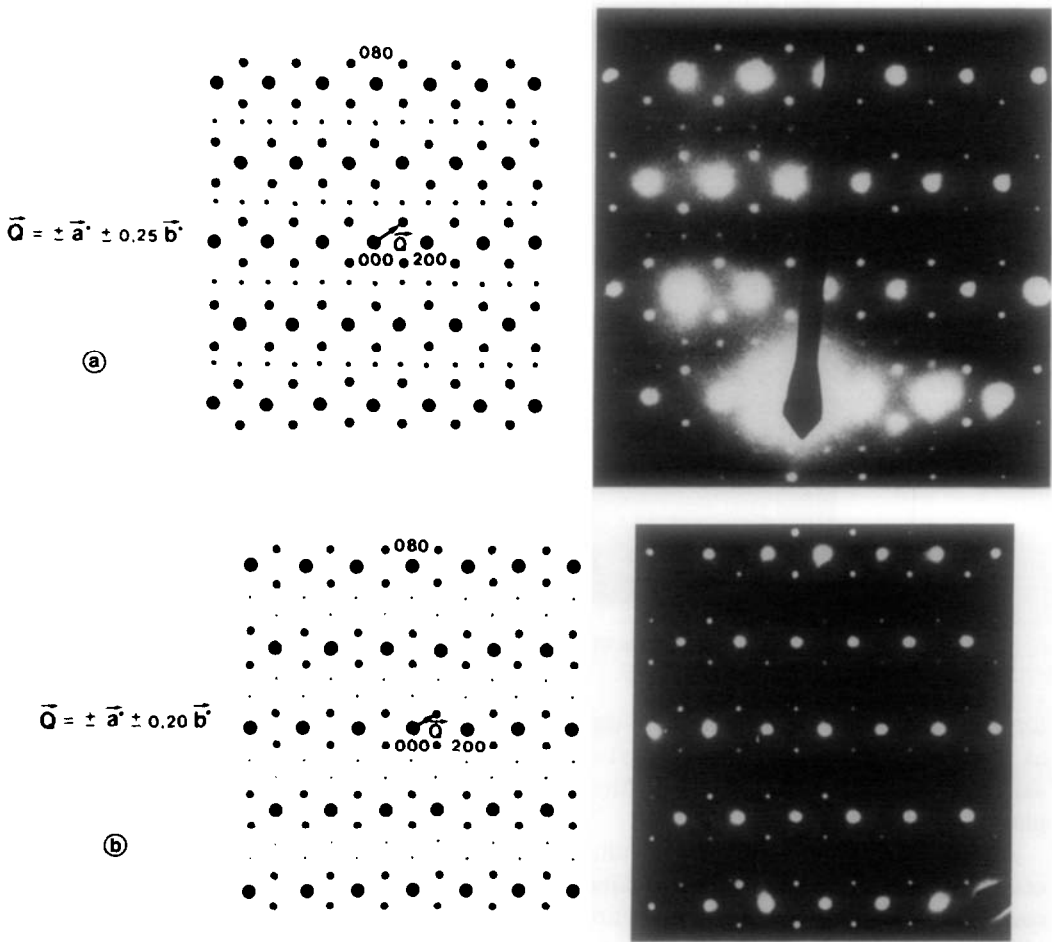


FIG. 3. Electron diffraction pattern: (001)\* plane of  $\text{Na}_{0.25}\text{TiO}_2$  types II and III; (a) room temperature, (b)  $300 \text{ K} < T < T_c^{3D}$ .

filtered molybdenum radiation in order to reduce the exposure time (17 hr). A platelet-like type III crystal elongated along the  $b$ -axis was glued with refractory cement on

a quartz stick. A device built in Grenoble (19) permitted heating of the sample in an argon stream. Peaks positions were determined on films by use of a Nonius densi-

TABLE III

$hkl$		Lattice parameters				$q$ in $b^*$ units	Averaged linewidth ( $\times 3\omega$ ( $^\circ$ ))
Class	Number	$a$ ( $\text{\AA}$ )	$b$ ( $\text{\AA}$ )	$c$ ( $\text{\AA}$ )	$\beta$ ( $^\circ$ )		
$k = 1, 5, 9, \dots$	16	12.173(4)	15.55(1)	6.473(2)	107.02(3)	$0.2492 \pm 0.0005$	0.70(10)
$k = 3, 7, 11, \dots$	15	12.174(4)	15.446(8)	6.471(2)	107.03(3)	$0.2491 \pm 0.00045$	0.65(9)
$k = 4, 8, 12, \dots$	25	12.174(4)	15.499(4)	6.473(2)	107.00(3)		0.59(9)

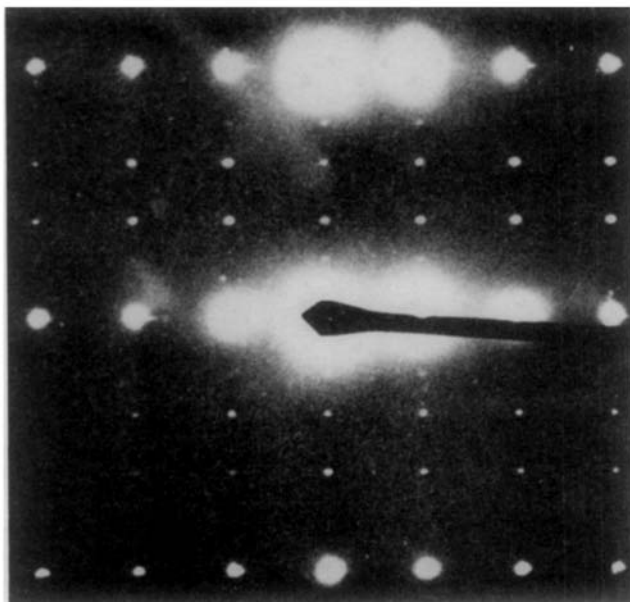


FIG. 4. (102)\* diffraction plane of  $\text{Na}_{0.25}\text{TiO}_2$  types II and III at room temperature.

tometer. For each temperature,  $q$  is defined as the length ratio between two first-order satellites and two Bragg peaks in the  $hk0$  plane.

As temperature increases, the  $q$  value decreases (Fig. 6). The  $q$  values obtained at room temperature by both methods are significantly different,  $0.243 \pm 0.001$  and  $0.24915 \pm 0.0005$ , respectively, by the precession method and the four-circle diffractometer. This discrepancy may arise for an intrinsic reason, due to small differences in composition between the crystals, or to an extrinsic one, due to experimental methods.

Twenty-five Bragg reflections were used to determine the thermal behavior of the cell parameters on a Philips three-circle diffractometer. Two transitions are clearly noted, in good agreement with the results obtained either by DSC ( $T_c^{3D} = 430$  K) or by electronic conductivity and magnetic measurements ( $T_p = 630$  K) (15). These are shown in Fig. 7. The main feature to be noted is the decrease in  $b$  as the tempera-

ture increases; this may be correlated with the metallic conductivity observed above 630 K. If one considers a linear extrapolation of parameters from the low temperatures (dotted line on Fig. 7) it appears that the relative variation of the  $b$ -axis is about  $-0.47 \pm 0.01\%$ , as compared to  $+0.34 \pm 0.01\%$  for  $a$ - and  $c$ -axes at 630 K.

The integrated intensities of the satellite peaks are proportional to the square of the order parameter ( $I\alpha\eta^2$ ). The five strongest satellite peaks 651, 652,  $\bar{7}12$ , 631, and 433 have been measured in the temperature range 130–450 K. Four Bragg peaks  $\bar{7}41$ , 683, 542, and 802 of quite similar intensity with those of satellite peaks are used as standards. The relative precision for the standard determination is roughly 3%. Measurements are reproducible on temperature cycling. All the satellite peaks exhibit the same thermal behavior. The variation of the order parameter,  $\eta$  versus temperature, as calculated from the average normalized intensities is shown in Fig. 8. The smooth variation is in agreement with a second-or-

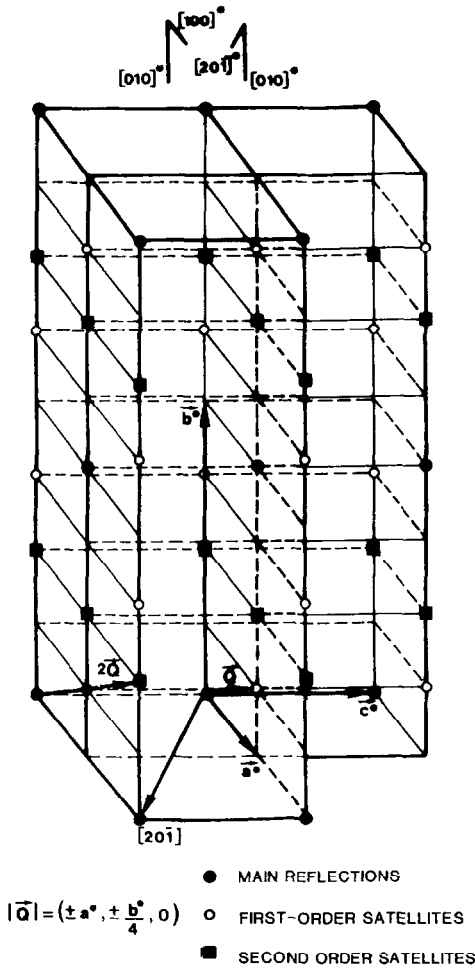


FIG. 5. Three-dimensional lattice of the commensurate phase in reciprocal space.

der transition. Near 430 K, the curve may be fitted (full line on Fig. 8) by  $\eta = a(T_c - T)^\beta$  with  $a = 0.223$  and  $\beta = 0.324$ .

This critical exponent  $\beta$  is in good agreement with the one determined by the renormalization group method for a dimensionality  $d = 3$  and  $n = 1$  ( $n =$  number of components of order parameter), namely,  $\beta = 0.325 \pm 0.0015$  (16).

Near 430 K, the long-range order disappears, as illustrated in Fig. 9, by the variation of the 651-reflection profile with temperature.

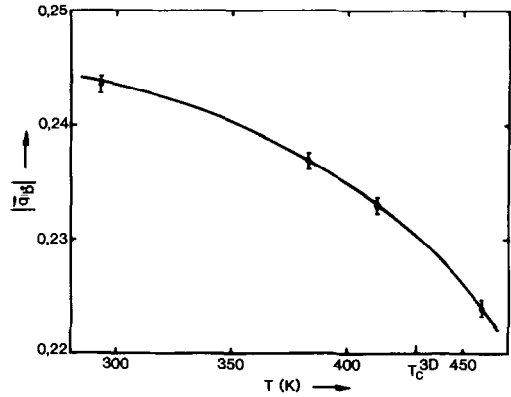


FIG. 6.  $q$  component of wave vector in  $b^*$  units versus temperature.

**Conclusion**

This study enables a comparison to be made of the bronzes Na<sub>0.21</sub>TiO<sub>2</sub> and Na<sub>0.25</sub>TiO<sub>2</sub>. The former does not exhibit anomalous specific heat when the temperature increases. By contrast, the latter undergoes a

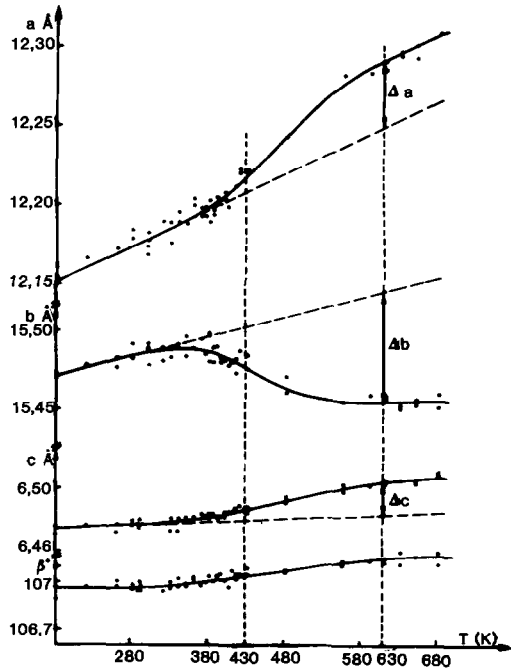


FIG. 7. Thermal behavior of cell parameters.

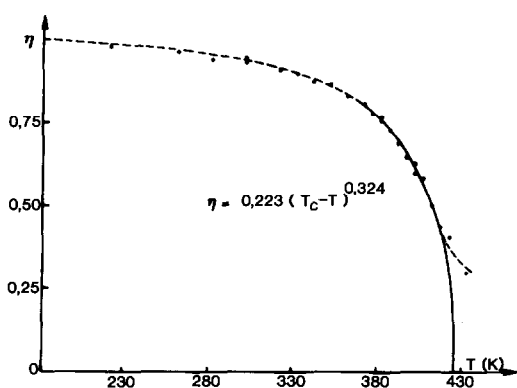


FIG. 8. Order parameter  $\eta$  versus temperature.

second-order transition in relation to the stoichiometry  $x = 0.25$ . For lower  $x$  values there is a sodium disorder inside the channel parallel to  $\mathbf{b}$ ; it is likely that such a disorder destroys the long-range lattice distur-

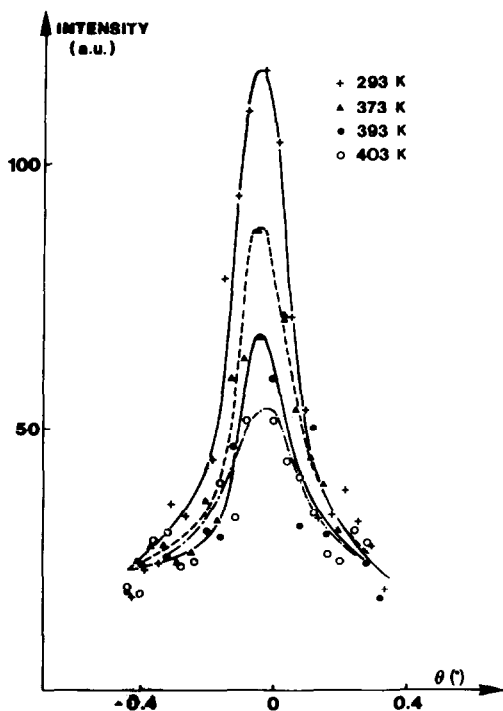


FIG. 9. Temperature dependence of the 651-supersubstructure reflection profile.

tion which appears for  $x = 0.25$  in the low-temperature range.

For  $\text{Na}_{0.25}\text{TiO}_2$  the critical exponents  $\alpha$  and  $\beta$ , related to the second-order transition at  $T_c^{3D} = 430$  K, have been determined. The wave vector  $\mathbf{Q}$  has been measured at room temperature. Its  $q$  component along  $\mathbf{b}^*$  decreases with increasing temperature. This behavior characterizes a displacive modulation which arises from Peierls transition at  $T_p = 630$  K. Due to strong electron-phonon coupling, the modulation of the lattice is accompanied by a simultaneous modulation of the electronic gas, forming a charge density wave with the wave vector  $2k_F$  along the  $\mathbf{b}^*$ -axis. At 430 K this charge density wave becomes static and orders three dimensionality.

From X-ray data collection at 135 K, a commensurate modulated structure determination is in progress using the concept of the four-dimensional space group.

## References

1. M. J. SIENKO, "Nonstoichiometric Compounds," *Advances in Chemistry Series*, p. 224, Amer. Chem. Soc., Washington DC (1963).
2. P. HAGENMULLER, "Progress in Solid State Chemistry," Vol. 5, p. 71, Pergamon, New York (1971).
3. P. G. DICKENS AND P. J. WISEMAN, *Solid State Chem.*, p. 211 (1974).
4. J. DUMAS, C. SCHLENKER, J. MARCUS, AND R. BUDER, *Phys. Rev. Lett.* **50**, 757 (1983).
5. J. POUGET, S. KAGOSHIMA, C. SCHLENKER, AND J. MARCUS, *J. Phys. (Paris) Lett.* **44**, L113 (1983).
6. M. GANNE, A. BOUMAZA, M. DION, AND J. DUMAS, *Mater. Res. Bull.* **20**, 1297 (1985).
7. D. C. JOHNSTON, H. PRAKASH, W. H. ZACHARIASEN, AND R. VISWANATHAN, *Mater. Res. Bull.* **8**, 777 (1973).
8. D. C. JOHNSTON, *J. Low-Temp. Phys.* **25**, 145 (1976).
9. M. R. HARRISON, P. P. EDWARDS, AND J. B. GOODENOUGH, *J. Solid State Chem.* **54**, 136 (1984).
10. M. R. HARRISON, P. P. EDWARDS, AND J. B. GOODENOUGH, *J. Solid State Chem.* **54**, 426 (1984).



11. A. D. WADSLEY AND S. ANDERSSON, *Nature (London)* **192**, 551 (1961).
12. S. ANDERSSON AND A. D. WADSLEY, *Acta Crystallogr.* **15**, 201 (1962).
13. A. F. REID AND M. J. SIENKO, *Inorg. Chem.* **6**(2), 321 (1967).
14. L. BROHAN AND R. MARCHAND, *Solid State Ionics* **910**, 419 (1983).
15. L. BROHAN, R. MARCHAND, AND M. TOURNOUX, to be published.
16. J. C. LE GUILLOU AND I. ZINN-JUSTIN, *Phys. Rev. B* **21**, 9 (1980).
17. J. P. POUGET, "Solid State Phase Transformation in Metals and Alloys," p. 223, (France) Ed. de Physique, Aussois (1980).
18. B. GALLOIS, J. GAULTIER, T. GRANIER, R. AYROLES, AND A. FILHOL, *Acta Crystallogr. B* **41**, 56 (1985).
19. R. ARGOUT AND J. J. CAPPONI, *J. Appl. Crystallogr.* **17**, 420 (1984).